

The cone inputs to the unique-hue mechanisms

Sophie M. Wuerger^{a,*}, Philip Atkinson^b, Simon Cropper^c

^a Centre for Cognitive Neuroscience, School of Psychology, University of Liverpool, Liverpool, UK

^b The Neurosciences Research Institute, School of Life and Health Sciences, Aston University, Birmingham, UK

^c Department of Psychology, University of Melbourne, Vic., 3010, Australia

Received 10 December 2004; received in revised form 17 May 2005

Abstract

Our aim was to characterise the chromatic mechanisms that yield the four unique hues: red, green, yellow and blue. We measured the *null planes* for all four unique hues and report the following two main results. (1) We confirm that three chromatic mechanisms are required to account for the four unique hues. These three chromatic mechanisms do not coincide with the chromatic tuning found in parvocellular LGN neurones, i.e., neurones tuned to L–M and S–(L+M); these subcortical chromatic mechanisms are hence not the neural substrate of the perceptual unique hues and further higher-order colour mechanisms need to be postulated. Our results are consistent with the idea that the two higher-order colour mechanisms that yield unique red and unique green respectively combine the incremental and decremental responses of the subcortical chromatic mechanisms with different weights. In contrast, unique yellow and unique blue can be explained by postulating a single higher-order chromatic mechanism that combines the incremental and decremental subcortical chromatic responses with similar weights. (2) The variability between observers is small when expressed in terms of perceptual errors, which is consistent with the hypothesis that the colour vision system in adult humans is able to recalibrate itself based on prior visual experience.

© 2005 Elsevier Ltd. All rights reserved.

Keywords: Colour; Vision; Psychophysics; Cone; Cortex

1. Introduction

When human observers are asked to adjust a coloured light such that it appears neither red nor green, or such that it appears neither yellow nor blue, most colour-normal observers have no difficulty in making these adjustments (Valberg, 1971) and these colour appearance judgements are not influenced by culture and language (Saunders & van Brakel, 1997), or by age (Kuehni, 2001; Scheffrin & Werner, 1990). This suggests that there is something very fundamental about these four attributes: redness, greenness, yellowness and blueness. However, despite their perceptual distinctiveness

and invariance, no clear rationale for the organisation of human colour vision into these four unique hues has emerged. An evolutionary approach has been successful to explain some aspects of human colour vision (Mollon, 1991), but it cannot account for the existence of the unique hues. More recently, Purves, Lotto, and Polger (2000) have argued that the four unique hues are optimal in distinguishing spectral boundaries. However, to date, no representative analysis of spectra has been performed to evaluate the extent to which unique hues are optimal categories in natural scene analysis. All attempts to identify the neural processes underlying the unique hues have failed (Mollon & Jordan, 1997) and it is still unclear how the known colour-opponent processes relate to the unique hues.

The aim of the present paper is not to ask ‘why’ human colour vision is, at least at one level, organised in

* Corresponding author. Tel.: +44 151 794 2173; fax: +44 151 794 2967.

E-mail address: s.m.wuerger@liverpool.ac.uk (S.M. Wuerger).

terms of unique hues, but rather to identify 'how' the receptor signals are combined in the brain to yield the unique hues. An understanding of the mapping from the retina to the brain might help us to identify the neural structures that compute these unique hues and might help us to get insight into the functional significance of these fundamental colour categories.

Human colour vision depends on several stages of processing. First, the light is absorbed by the long-, medium- and short-wavelength-sensitive (L-, M-, or S-) cone receptors (Helmholtz, 2000). Then the cone outputs are recombined in post-receptoral channels. The early stages of this re-combination of the cone outputs are well understood and have been confirmed in neurophysiological studies (Derrington, Krauskopf, & Lennie, 1984; De Valois, Cottaris, Elfar, Mahon, & Wilson, 2000; De Valois & De Valois, 1993). These experiments suggest that the first stage of post-receptoral encoding corresponds to two chromatic mechanisms, one of them taking the difference between the L and the M cones ('L–M mechanism'), the other one taking the differences between the summed L and M cones and the S cones ('S–(L+M) mechanism'). These cardinal cone-opponent colour directions are often loosely referred to as red–green and yellow–blue colour directions. Although some behavioural experiments employing adaptation (e.g., Wuerger, 1996) and habituation (e.g., Krauskopf, Williams, & Heeley, 1982; Zaidi, Yoshimi, Flanagan, & Canova, 1992) paradigms or similarity measures (Maloney, Wuerger, & Krauskopf, 1994; Wuerger, Maloney, & Krauskopf, 1995) confirm that these are important and salient colour mechanisms, the cardinal directions do not map readily onto the perceptually 'unique hue' sensations (Barbur, Harlow, & Plant, 1994; De Valois, De Valois, Switkes, & Mahon, 1997; Gegenfurtner, Kiper, & Levitt, 1997; Kiper, Fenstemaker, & Gegenfurtner, 1997; Valberg, 1971; Webster, Miyahara, Malkoc, & Raker, 2000a; Webster, Miyahara, Malkoc, & Raker, 2000b; Webster et al., 2002).

'Unique hues' were first mentioned by Hering (1964) who proposed that any hue can be described in terms of its redness or greenness and its yellowness or blueness. Red and green are opposite hues because they cannot be elicited simultaneously by a single colour stimulus; the same is true for blue and yellow. This observation led Hering to postulate the existence of two opponent channels coding red–green and yellow–blue sensations. Jameson and Hurvich (1955) used a hue cancellation technique to determine the unique hues experimentally. Observers viewed a small test stimulus on a white surround and adjusted the test light until it looked 'neither red nor green' (yielding 'unique yellow' and 'unique blue') or 'neither yellow nor blue' (yielding 'unique red' and 'unique green'). The idea is that unique yellow and unique blue are obtained by silencing a red–green mechanism, hence 'unique yellow' and 'unique

blue' are often referred to as 'red–green equilibria'. Similarly, unique red and unique green are referred to as 'yellow–blue equilibria' since the assumption is that for these unique hues the opponent yellow–blue mechanism is in equilibrium (Hurvich & Jameson, 1955; Ingling, Russell, Rea, & Tsou, 1978; Jameson & Hurvich, 1955; Valberg, 2001).

To further characterise the properties of the equilibria-mechanisms that yield the unique hues, Larimer and colleagues tested their linearity. Direct tests on the homogeneity of the unique hues revealed that unique green, unique blue and unique yellow are invariant under moderate luminance changes (Knoblauch, Sirovich, & Wooten, 1985; Larimer, Krantz, & Cicerone, 1974; Larimer, Krantz, & Cicerone, 1975). Small deviations from this proportionality law were found for unique red (Larimer et al., 1975). Additivity was tested by adding hues that were neither red nor green, i.e., unique yellow or unique blue, and testing whether the resulting stimulus was again neither red nor green, i.e., unique yellow or unique blue. Additivity holds for unique yellow and for unique blue (Cicerone, Krantz, & Larimer, 1975), but consistent failures of additivity are found for uniquely red and uniquely green lights (Burns, Elsner, Pokorny, & Smith, 1984b; Ikeda & Ayama, 1980; Werner & Wooten, 1979). Cicerone et al. (1975) tested whether the linearity laws for unique hues hold under moderate changes in adaptation and found nonlinearities for the unique red and unique green stimuli under a variety of chromatic adaptation conditions. Larimer and colleagues concluded that the yellow–blue mechanism (yielding unique red and unique green) is non-linear in cone space. More recently, researchers noticed that the consistent failure of linearity for unique red and unique green can simply be accounted for by assuming not *one* red–green mechanism but *two* different mechanisms, a red and a green mechanism, both mechanisms having the neutral grey as an origin (Chichilnisky & Wandell, 1999; Mausfeld & Niederee, 1993).

With recent advances in understanding the cortical mechanisms of colour vision (De Valois et al., 2000; Johnson, Hawken, & Shapley, 2001), the 'unique hues' have remained a mystery. Neither neurophysiological studies with monkeys (Lee, Wachtler, & Sejnowski, 2002; Wachtler, Sejnowski, & Albright, 2003) nor functional imaging studies with humans (Morita et al., 2004; Wandell et al., 1999) have revealed neurones with chromatic tuning similar to the unique hues. Neurones tuned to directions other than the cardinal cone-opponent axes have been found in striate (Lennie, Krauskopf, & Schlar, 1990) and extrastriate areas of the visual cortex (Kiper et al., 1997) but the unique hues do not seem to have a special status.

The main aim of this study was to establish the differential cone inputs to the mechanisms that yield the four unique hues. Using a psychophysical hue selection task,

we obtained data (in three-dimensional cone space) of all four unique hues. To obtain a representative mapping, we tested a large sample of colour-normal observers and measured the unique hues for a wide range of luminance and saturation levels. We also tested whether a piecewise linear model (in three-dimensional cone space) provides a satisfactory account of the cone inputs to the unique hues. We found this to be the case hence confirming earlier studies (Chichilnisky & Wandell, 1999; Mausfeld & Niederee, 1993). Establishing the precise cone inputs to the unique hues psychophysically will be useful in guiding imaging and neurophysiological studies in the quest for neurones with a chromatic tuning similar to the unique hues.

2. Methods

2.1. Determining unique hues using a hue selection task

In preliminary experiments, we found that the hue selection task was faster and easier for the observers than obtaining the unique hue data via cancelling the opponent colours by method of adjustment. We therefore employed a hue selection task to obtain data for the unique hues for a wide range of luminance and saturation levels.

Each trial in this hue selection task consisted of two stages; only the response at the second stage was included in the data. At the beginning of each trial a message appeared on the screen telling the observer to provide a selection for a particular unique hue, e.g., for unique red. Then an annulus consisting of 12 coloured disks covering the entire hue circle was presented hence containing a very coarse hue spectrum. Each individual disk had a diameter of 1.5° of visual angle; the radius of the annulus was 5° and was centered at the midpoint of the screen; on each trial the colour was assigned randomly to a particular patch on the annulus. The observer made a selection by clicking with the mouse on the coloured patch, which is closest to unique red. Then a 'zoomed-in' version of the hue annulus was presented consisting of coloured patches centered on the first selected hue, some patches containing more yellow some more blue. The exact hue range and hue spacing used in the second presentation was determined in a pilot study. Now the observer made the final hue selection by mouse click.

The data for unique green, yellow and blue were derived in a similar manner. Unique green was established by showing a range of greenish coloured disks and the observer was asked to pick the disk that looked 'neither yellow nor blue'. Unique yellow and unique blue were determined by asking observers to choose the disk that contained 'neither red nor green'. All observers found the task easy and did not need require any further instructions or any explanations what 'neither red not green' (or 'neither yellow nor blue') meant.

In each session all four unique hues were determined at different saturation and luminance levels. Internally, saturation and luminance levels were specified in terms of hue-saturation-value (HSV) space (Travis, 1991, pp. 81ff). This colour space is convenient for stimulus selection since we attempted to keep the saturation and the luminance level approximately the same for all the colour patches presented on a particular trial; this facilitates the task of the observer to select the most appropriate hue. The HSV space is scaled such that it makes use of the entire monitor gamut. 'Value' (which is loosely related to luminance) can range from 0 to 1; 0 is black and 1 is white (for an achromatic colour). Saturation can range from 0 to 1 and refers to the amount of grey in a particular colour; a saturation of 0 indicates a grey colour; a saturation of 1 refers to a fully saturated colour. Hue is specified as an angle ranging from 0 to 360 deg. Based on preliminary experiments, we used saturation levels ranging from 0.2 to 1.0, in steps of 0.05, and value levels ranging from 0.3 to 1.0, again in steps of 0.05. These value levels resulted in luminances ranging from 2 to 130 cd/m^2 , with an average luminance of about 42 cd/m^2 . At a particular trial, a specific combination of saturation and level was used; the order of presentation was randomised.

For each trial, the saturation and value level together with the chosen hue angle was stored. These (device-dependent) HSV co-ordinates were first converted to (device-dependent) RGB space and then to LMS cone space (for details see Travis, 1991). The co-ordinates in LMS space are given in the result section (Fig. 3(A)–(D)).

2.2. Apparatus and procedure

All stimuli were presented on a CRT screen of a DELL monitor (DELL P790). Linearised look-up tables were produced by measuring the CRT light outputs with a spectroradiometer (SpectraScan PR650; PhotoResearch). The background was always grey with a mean luminance of 43 cd/m^2 and with chromaticity co-ordinates $x = 0.282$ and $y = 0.307$. The observers were seated in a darkened room 1 m away from the monitor and adapted to the grey background for at least 5 min. The stimuli were presented continuously until the observer responded. There was no time limit for the response and the observers were encouraged to move their eyes freely.

All observers were tested with the Cambridge Colour Vision Test and only observers with colour-normal results were used for the unique hue experiment. Eighteen observers took part in the unique hue experiment. Most of them were undergraduate students in Neuroscience, Psychology or Computer Science; one observer was one of the authors. Eleven of the 18 observers were female; the age ranged from 20 to 39.

For each observer and in each session all four unique hues were determined at different luminance and saturation levels (see Section 2). Each observer made at least 80 selections for each unique hue. Altogether, for each unique hue we obtained 1616 data points.

3. Results

Each unique hue selection is a point in a three-dimensional space defined by the absorptions of the three different cone classes (Long-wavelength- (L), medium-wavelength- (M) and short-wavelength- (S) sensitive cones). To visualise the loci of the unique hues in a two-dimensional space, we first present our data in the cone-opponent mechanisms space (DKL space; Derington et al., 1984). DKL space is a linear transformation of LMS space and for our chosen background colour the transformation is given by

$$\begin{bmatrix} \Delta L + \Delta M \\ \Delta L - \Delta M \\ \Delta S - (\Delta L + \Delta M) \end{bmatrix} = \begin{bmatrix} 0.0399 & 0.0399 & 0 \\ 0.0264 & -0.0473 & 0 \\ -0.0230 & -0.0230 & 1.0703 \end{bmatrix} \begin{bmatrix} \Delta L \\ \Delta M \\ \Delta S \end{bmatrix}$$

On the right-hand side are the differential cone absorptions, which are obtained by subtracting the background cone absorptions from the absolute stimulus cone absorptions. On the left-hand side are the corresponding cone-opponent mechanisms co-ordinates. For the sake of simplicity we refer to them as luminance, ‘ $\Delta L - \Delta M$ ’, and ‘ $\Delta S - (\Delta L + \Delta M)$ ’. We scale the matrix such that a unit vector in cone contrast space ($\Delta L/L_{BG}$, $\Delta M/M_{BG}$, $\Delta S/S_{BG}$) produces a unit response in each of the mechanism (Brainard, 1996; Wuerger, Watson, & Ahumada, 2002). This scaling is to some extent arbitrary, but it does not affect our conclusions. We only use DKL space to visualise the data and make comparisons to previously published data; the main data analysis will be performed in three-dimensional LMS space.

Fig. 1 shows the ‘ $\Delta L - \Delta M$ ’, and ‘ $\Delta S - (\Delta L + \Delta M)$ ’ co-ordinates of the unique hues; red symbols (circles) refer to the data for ‘unique red’ and green symbols (squares) to ‘unique green’; yellow symbols (upward pointing triangles) denote the data for ‘unique yellow’ and blue symbols (downward pointing triangles) indicate the loci of ‘unique blue’. This figure illustrates two important properties of the unique hues. Firstly, it is clear that the unique hues do not coincide with the cardinal axes of DKL space confirming results by Webster and colleagues (2000b). Unique red is closer to the positive end of the ‘ $L - M$ ’ axis, whereas unique green clearly needs a significant negative S-cone contribution. This means that the green that constitutes the negative end of the ‘ $L - M$ ’ axis is too bluish to be considered in yellow–blue equilibrium. Similarly, the red on the positive

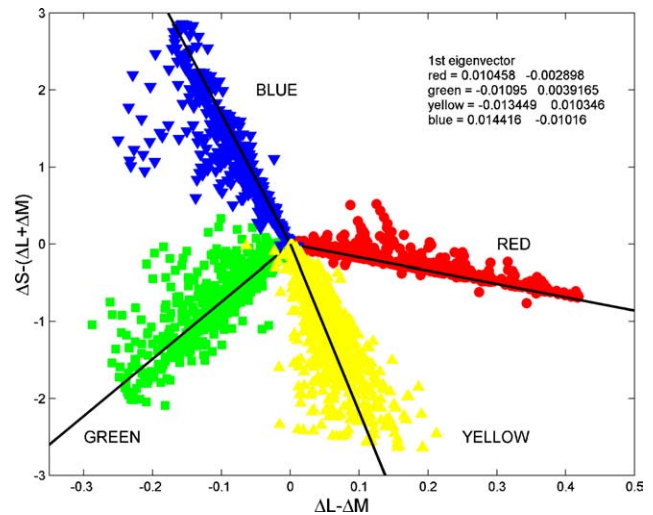


Fig. 1. The four unique hues in DKL space. 1616 data points are shown for each unique hue. Red symbols (circles) denote data for ‘unique red’, green symbols (squares) for ‘unique green’, yellow symbols (upward pointing triangles) for ‘unique yellow’ and blue symbols (downward pointing triangles) for ‘unique blue’. The solid black lines indicate the first eigenvector for each unique hue (see Section 4 for further details). (For interpretation of the references to colour in this figure legend, the reader is referred to the web version of this article.)

end of the ‘ $L - M$ ’ axis also needs S-cone input to silence the putative yellow–blue mechanism. Unique blue is not even close to the positive end of the $S - (L + M)$ axis: S-cone-isolating stimuli appear violet and not blue. Unique blue needs a significant negative $L - M$ input, whereas unique yellow requires a positive $L - M$ input. The negative endpoint of the $S - (L + M)$ axis looks greenish, not yellow. The second important feature is that unique red and unique green do not lie on a line through the origin. This implies that it is not a single opponent yellow–blue mechanism, which is silenced when observers consider a light being neither yellow nor blue. There are two possibilities to explain this lack of co-linearity: either a single but very nonlinear YB mechanism is silenced or two separate, but piecewise linear YB mechanisms. We will come back to this issue later in the model section. The results for unique yellow and unique blue are different. To a first approximation, the loci of unique yellow and blue lie on a line through the origin suggesting that these colours may be generated by silencing a single red–green mechanism. We will test this hypothesis below.

The aim of this study was to determine how the individual cone signals contribute to the mechanisms that yield the unique hues, i.e., we attempt to find the mapping between LMS cone space and the chromatic mechanisms that are silenced by the respective unique hues. In Fig. 2(A), each individual unique hue selection is plotted as a data point in a space spanned by the differential L, M, S cone absorptions. The differential cone

absorptions are obtained by subtracting the background cone absorptions from the absolute cone absorptions. The symbols are as in Fig. 1: red symbols (circles) for ‘unique red’ and green symbols (squares) for ‘unique green’; yellow symbols (upward pointing triangles) for ‘unique yellow’ and blue symbols (downward pointing triangles) for ‘unique blue’.

To get a clearer picture of the loci of the four unique hues in LMS space, Fig. 2(B)–(D) shows the three two-dimensional sub-planes. Fig. 2(B) shows that with an increase in saturation, the L to M cone ratio for the unique hues, in particular for unique yellow and unique blue, is constant at 2:1. This L:M slope of 2:1 is reflected in the estimates shown in Table 1 which will be discussed in the next section; here the coefficients for the normal vector orthogonal to the unique hue planes are shown

and the ratio between the L and M cone coefficients is about 1:–2; this ratio describes the direction of the vector normal to the unique blue and yellow plane, rather than the orientation of the plane itself. Such a constant slope is not seen for unique red and unique green, which already suggests that unique red and green cannot be generated by a single chromatic mechanism (with identical L and M cone weights for unique red and green). This is reflected in the estimated coefficients shown in Table 1, which will be explained in the next section: unique red is characterised by a normal vector with an L:M cone ratio of about 1:–6, whereas the normal vector for the unique green plane requires an L:M cone ratio of about 2:–3. Fig. 2(C) and (D) reveals that unique yellow requires a mostly negative S cone input and unique blue a mostly positive S cone input.

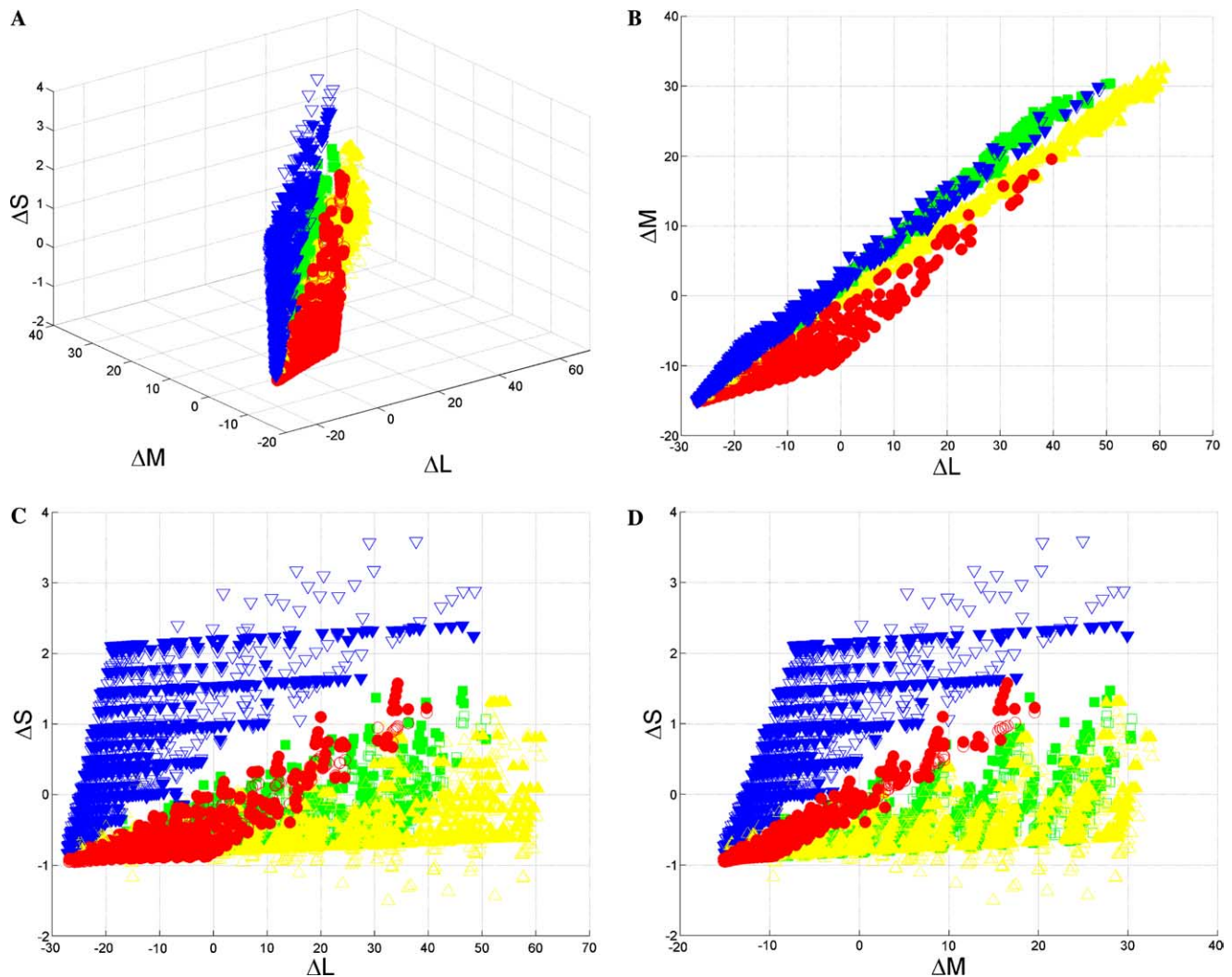


Fig. 2. (A). The four unique hues in LMS space. Red symbols (filled circles) denote data for ‘unique red’, green symbols (filled squares) for ‘unique green’, yellow symbols (filled upward pointing triangles) for ‘unique yellow’ and blue symbols (filled downward pointing triangles) for ‘unique blue’. The open symbols are the predicted loci based on a linear model (see text for details). (B)–(D) The filled symbols show the loci of the unique hues in the two-dimensional planes defined by the differential L, M, S cones respectively; the open symbols are the predictions based on a linear model (see below for details). Please note the ‘jumps’ in the unique hue data are a consequence of the hue sampling in the hue selection task (see Section 2). (For interpretation of the references to colour in this figure legend, the reader is referred to the web version of this article.)

Table 1

This table contains the coefficients (and standard deviations) for the chromatic mechanisms that are **silenced** by the unique hues and the corresponding summed squared error (in LMS space)

Unique Hue		L coefficient α	M coefficient β	S coefficient γ	Error SSQE
RED	<i>indiv</i>	0.0137 (0.0065)	−0.0863 (0.0099)	−0.9961 (0.0009)	3.60
	pooled	0.0131	−0.0857	−0.9962	8.41
GREEN	<i>indiv</i>	0.1966 (0.0278)	−0.2931 (0.0498)	−0.9337 (0.0201)	21.20
	pooled	0.1972	−0.2953	−0.9348	66.92
YELLOW	<i>indiv</i>	0.3316 (0.0636)	−0.6338 (0.1075)	0.6632 (0.1816)	55.65
	pooled	0.2875	−0.5467	0.7864	126.46
BLUE	<i>indiv</i>	0.2768 (0.0155)	−0.5384 (0.0331)	0.7947 (0.0259)	31.53
	pooled	0.2719	−0.5265	0.8055	58.72
R + G	<i>indiv</i>				1041.9
	pooled				1125.6
Y + B	<i>indiv</i>				159.73
	pooled				196.69

The coefficients α , β , γ (defined in Eqs. (1) and (2)), for the three cone classes are shown for all four unique hues. For example, the first row contains the coefficients of the mechanism that is silenced by all colours that are classified as ‘unique red’. The first row contains the mean coefficient for each cone class. Each mean coefficient is obtained by fitting the data for each observer individually (‘*indiv*’) and then averaging over all 18 observers. The standard deviation is shown in parentheses. The last column contains the sum of the squared deviations between the predicted (the fitted plane) and the observed LMS values. Below are the coefficients based on the pooled data over all observers (‘*pooled*’) with the associated error. For three unique hues (red, green, and blue) the coefficients based on individual data and the coefficients based on the pooled data are virtually identical. This suggests that there is very little variability between observers. For unique yellow, the mean coefficient and the coefficients based on the pooled data are slightly different which suggests that observers are more variable in their unique yellow judgements.

3.1. Characterising the cone inputs to the equilibria mechanisms

The main assumption in the hue cancellation task (or hue selection task) is that each unique hue is generated by silencing a chromatically opponent mechanism. For instance, all colours that are judged as ‘unique red’ appear ‘neither yellow nor blue’. Hence, we postulate that there exists a yellow–blue (YB) mechanism, which is silenced by unique red. Furthermore, if unique red (R) is generated by silencing a YB mechanism that combines the cone signals linearly, then we can write

$$\alpha_R * \Delta L + \beta_R * \Delta M + \gamma_R * \Delta S = YB_R = 0. \quad (1)$$

Eq. (1) defines a plane (through the origin) in three-dimensional cone space. The vector $(\alpha_R, \beta_R, \gamma_R)$ is orthogonal to this plane. This normal vector $(\alpha_R, \beta_R, \gamma_R)$ characterises the yellow–blue mechanism (YB_R) that is silenced by all the (unique red) colours on this plane. This plane is therefore the *null plane for the YB mechanism*. We can derive an analogous equation for unique green.

For unique yellow we assume that a particular red–green mechanism (RG_Y) is silenced since unique yellow is obtained by selecting a yellowish light that appear ‘neither red nor green’. The null plane for this opponent RG mechanism is therefore defined as

$$\alpha_Y * \Delta L + \beta_Y * \Delta M + \gamma_Y * \Delta S = RG_Y = 0. \quad (2)$$

The vector $(\alpha_Y, \beta_Y, \gamma_Y)$ is orthogonal to this plane and characterises the red–green mechanism (RG_Y), which is silenced by all colours on this plane. An analogous null plane can be derived for unique blue; the corre-

sponding normal vector characterises the red–green mechanism (RG_B), which is silenced by all colours on this null plane.

We can now ask the following questions: (1) Do these chromatic ‘equilibrium’ mechanisms (RG, YB) combine the cone signals linearly and what are the coefficients (α , β , γ) for each of the four unique hues? (2) Are unique red and unique green generated by silencing a single YB mechanism or two different YB mechanisms (YB_R and YB_G)? Similarly, are unique yellow and unique green generated by silencing a single RG mechanism or two different RG mechanisms (RG_Y and RG_B)?

To test whether the chromatic mechanisms that are at equilibrium for the unique hues are linear combinations of the cone signals, we fit a plane to each of the four unique hue data. The respective normal vectors (Eqs. (1) and (2)) define the mechanisms that are silenced by the unique hues.

3.2. Fitting the null planes

For each unique hue, we determined the best-fitting plane (Eqs. (1) and (2)) by minimising the Euclidean distances between the individual unique hue co-ordinates (in LMS space) and the plane. This is often called a ‘Total Least Squares’ solution or ‘Orthogonal Distance Regression’ (Jobson, 1991) since orthogonal distances are minimised as opposed to distances along a single (usually Y) dimension, which is common in an ordinary regression problem with several independent variables and one dependent variable.

The constraint equation is of the form: $AB = 0$, where B is a column vector containing the coefficients (α, β, γ) and A is an $n \times 3$ matrix where each row contains the differential LMS co-ordinates of a unique hue selection $(\Delta L, \Delta M, \Delta S)$. The coefficients are normalised such that $\alpha^2 + \beta^2 + \gamma^2 = 1$. For each unique hue we fitted $n = 1616$ data points. Vector B is the normal vector for the fitted plane and its coefficients (α, β, γ) define the orientation of the chromatic mechanism, which is silenced by the particular unique hue, in LMS space. The coefficients (α, β, γ) correspond to the weighting of the respective differential L, M, S cone signals (see Eqs. (1) and (2)). An equivalent method for finding the coefficients (α, β, γ) is a principal component analysis (PCA). The last eigenvector (explaining the least variance) is the normal vector.

Fig. 3(A)–(D) shows the four unique hues with the null planes and corresponding normal vector. All four plots are scaled in the same way so that a comparison between the orientations of the four null vectors is possible.

The two main results are: (1) For all four unique hues the data are well fit by a plane suggesting that, for moderate luminances and saturations, the mechanisms that are in equilibrium for unique hues, combine the differential cone input linearly. (2) To obtain unique red and unique green we must postulate that two different YB mechanisms are at equilibrium. This is illustrated by different orientations of the normal vectors for unique red and green.

3.3. Unique red and unique green

Fig. 3(A) and Table 1 show that unique red is silencing a mechanism (YB_R), which is almost exclusively driven by the S cones. The normal vector (Fig. 3(A)) is almost parallel to the S cone axis, hence the null plane is parallel to the plane spanned by the L and M cones. This YB_R mechanism has a small, opponent L and M cone input in addition to very large S cone input. This is also reflected in the fact that, in Fig. 1, unique red lies

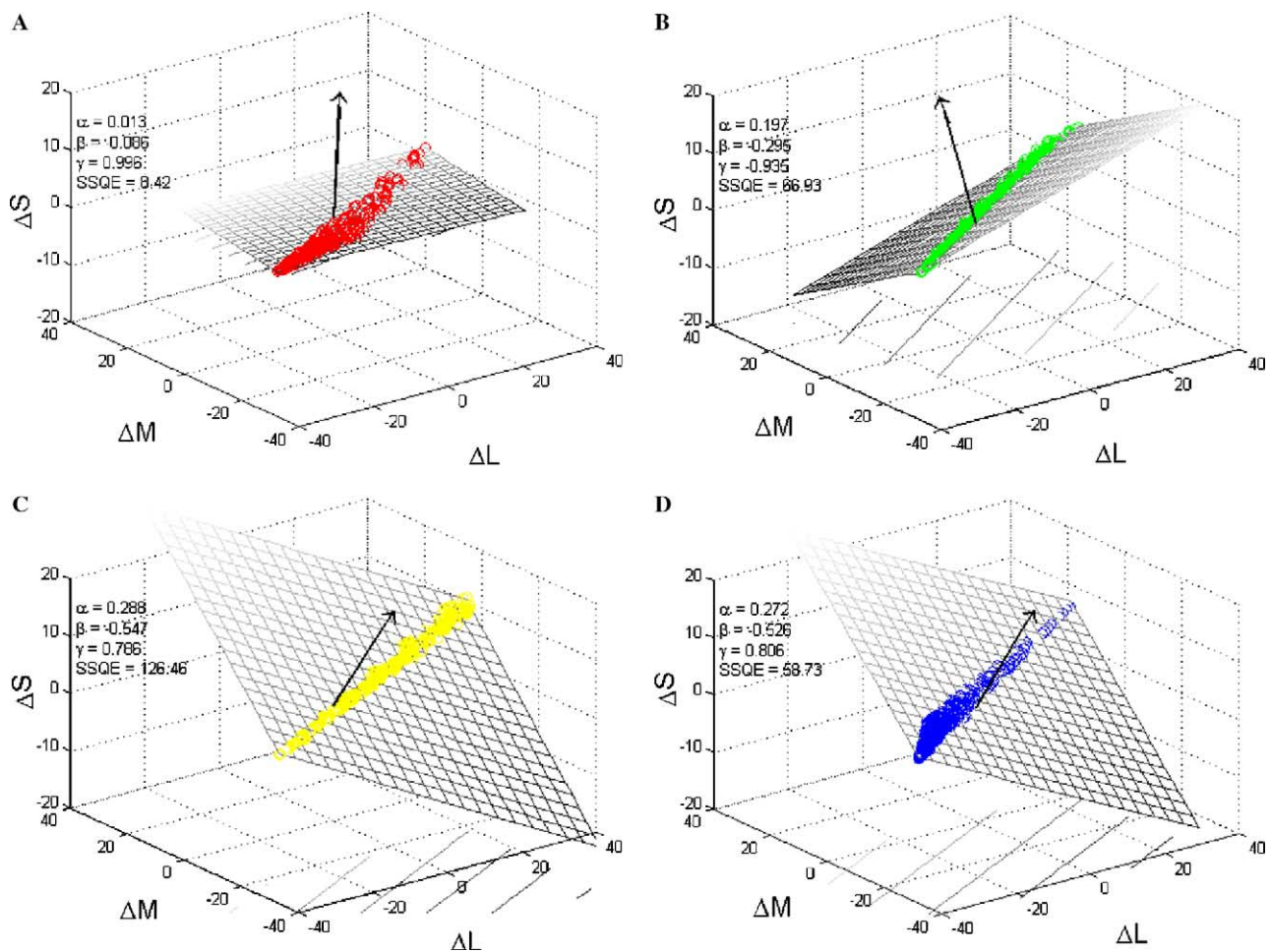


Fig. 3. Panels (A)–(D) show the four unique hues (red, green, blue, and yellow) with the null planes and corresponding normal vectors. Please note that the axes are scaled in order to visualise the orientations of the null planes and their associated normal vectors (i.e., the chromatic mechanisms that are silenced by the colours on the null plane); as a consequence the data are compressed to a very small range and seem to lie on a line. The range of the loci of the unique hues is better illustrated in Fig. 1.

fairly close to the L–M axis. Hence, a mechanism that has a null response to this hue, must have a large S cone input. The magnitude of the coefficients for L/M on one hand and the S cones on the other hand is not easy to compare since this depends on the scaling adopted for the L, M, S absorptions. The S cone absorptions are pretty small compared to the L and M absorptions (<2 ; see Figs. 2 and 3); therefore the S cone coefficients are bound to be rather large. However, it is meaningful to compare the S cone input across the different unique hues. Such a comparison reveals that the YB mechanism that is silenced by unique green (YB_G) requires a smaller S cone input and a larger (opponent) L–M cone input than YB_R. Comparing Fig. 3(B) with 3(A) shows that the null plane for unique green is clearly tilted and not parallel to the S cone axis, which reflects the significant S cone input to the YB mechanism that is silenced by unique green (see also Table 1). The different orientations of the null planes for unique red and unique green implies that these two unique hues cannot be generated by silencing a single YB mechanism. This can also be seen in Fig. 1 which shows a clear bend in the contour consisting of the unique red and green hues. The most parsimonious explanation is that two linear mechanisms are at work (with the grey background as the origin). This is confirmed by analysing the errors in Table 1. If unique red and green are the null planes for a single YB mechanism, then fitting both planes simultaneously should yield an error which is approximately the sum of the two individual errors (8.3 for red and 64.7 for green). The error for the combined fit, however, is 1108.5. We can hence reject the hypothesis that the same YB mechanism is silenced when human observers perceive colours as unique red and unique green. Unique red silences a chromatic mechanism which receives almost exclusively S cone input, whereas the second YB mechanism yielding unique green, receives significant opponent input from the L and M cones as well. Both YB mechanisms take the difference between an L–M cone and S cone inputs. Hence, we could refer to these YB mechanisms as ‘((L–M)–S)’. The individual cone weighting is different for the two yellow–blue mechanisms; the YB mechanism that is at equilibrium for unique red (YB_R) receives less L and M cone input than the mechanism that is silenced by unique green (YB_G).

The finding that yellow–blue equilibria colours, i.e., unique red and unique green, cannot be generated by a single chromatic mechanism is consistent with the conclusions reached by Larimer and his colleagues (Larimer et al., 1974; Larimer et al., 1975), employing a different task and a different method of analysis (cf. Fig. 5). We have shown that two linear mechanisms with different cone inputs can account for the loci of unique red and unique green, which is consistent with a piecewise linear model (Chichilnisky & Wandell, 1999).

3.4. Unique yellow and unique blue

Figs. 3(C) and (D) show the null planes for unique blue and yellow. The orientations of the null planes (and the corresponding normal vectors) are very similar. This is confirmed by the coefficients shown in Table 1. The putative red–green (RG) mechanism, which is silenced by unique yellow, receives a large opponent input from the L and M cones ($\alpha = 0.287$, $\beta = -0.546$) and, compared to the YB mechanisms, a relatively weak input from the S cones ($\gamma = 0.787$). The mechanism that is silenced by unique blue, has very similar cone inputs: a large, opponent input from the L and M cones ($\alpha = 0.272$, $\beta = -0.527$), and again, in comparison to the YB mechanisms, a relatively weak input from the S cones ($\gamma = 0.805$). In summary, the data for unique yellow and unique blue are consistent with the hypothesis that a single RG mechanism is at equilibrium for these unique hues. This single RG equilibrium mechanism sums up L–M and S cone inputs; hence we could refer to it as ‘((L–M)+S)’. This conclusion is in agreement with Larimer and colleagues (Larimer et al., 1974; Larimer et al., 1975) who have shown that red–green equilibria colours, i.e., unique yellow and unique blue, may be generated by a single chromatic mechanism (cf. Fig. 5 and Table 1).

3.5. Variability between observers

To evaluate how well the unique hues are fitted by our linear model (Eqs. (1) and (2)) and whether there are significant differences between the individual observers, we calculate the perceptual errors between the observed and the predicted unique hues for both the pooled data and for the fits based on the individual data. If there are large differences between observers in the loci of the unique hues, we expect the perceptual errors based on the pooled data (across all observers) to be much larger than the error based on the individually fitted data.

The observed and predicted data points are first transformed into $L^*a^*b^*$ Space, which is an approximately uniform colour space (Wyszecki & Stiles, 1982). In Lab Space, L^* is the luminance, a^* , and b^* are, respectively, red–blue, and yellow–blue chromaticities. For each data point, we compute the distance between the predicted point (i.e., the point on the plane closest to the data point) and the observed unique hue. Perceptual distances are calculated using the colour difference formula proposed by the CIE in 1994, since the CIE94 colour difference formula was developed to fit small colour differences (CIE, 1995; Zhu, Luo, & Cui, 2000).

Figs. 4(A) and (B) shows the error histograms for all four unique hues. In Fig. 4(A), the data were pooled across all observers and a single plane was fitted for each unique hue. The frequency of perceptual errors, that is,

the distances between the predicted and the observed unique hues, are shown for all unique hues. For all four unique hues almost all errors are below 5; a perceptual error of 5 is visible in side-by-side image comparisons (Engel drum & Ingraham, 1990). Fig. 4(B) shows the error histograms for the individually fitted data. In this case, a best-fitting plane was found for each observer individually. As in Fig. 4(A), the frequency of perceptual errors between the predicted and the observed unique hues are shown for all four unique hues. The errors for the individual fits are slightly smaller than for the fits based on the pooled data and most errors are below 3.

In Fig. 5, the mean perceptual errors (CIE 1994 Lab ΔE) for fits based on the pooled data (left) and for individual fits (right) are shown. Fitting the planes for each observer individually reduces the average perceptual error by a small amount only: by a factor of 1.7 for red, 1.6 for green, 1.9 for yellow, and 1.1 for blue. This suggests that the variability between observers is relatively small when expressed in terms of perceptual errors.

Fig. 5 also shows the mean perceptual error when the data for unique red and unique green are fitted by a single plane (RG). The average perceptual error assuming a single yellow–blue mechanism is clearly much higher than the average errors for red and green. This implies that different yellow–blue chromatic mechanisms are silenced when observers perceive a colour as uniquely red

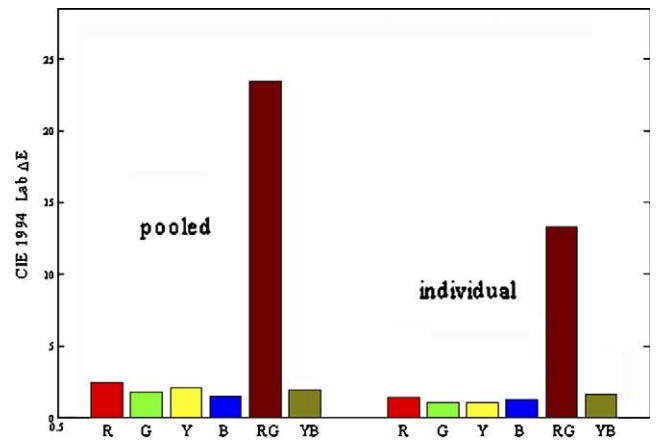


Fig. 5. The mean perceptual errors (CIE 1994 Lab ΔE) for fits based on the pooled data (left) and for individual fits (right) are shown. Fitting the planes for each observer individually reduces the average perceptual error by a small amount: by a factor of 1.7 for red, 1.6 for green, 1.9 for yellow, and 1.1 for blue. R, G, Y, B denote the four unique hues. When a single plane is fitted to the unique red and unique green data (RG), the average perceptual error is much larger than the sum of the R and G errors. This implies that no single mechanism is silenced by unique red and green, but two different mechanisms are at work. This holds for the pooled data and for the individual observer fits. In contrast, when a single plane is fitted to unique yellow and unique blue (YB), the average perceptual error is very similar to the errors for the separate fits. This is consistent with the hypothesis that unique yellow and unique blue are generated by silencing a single red–green mechanism.

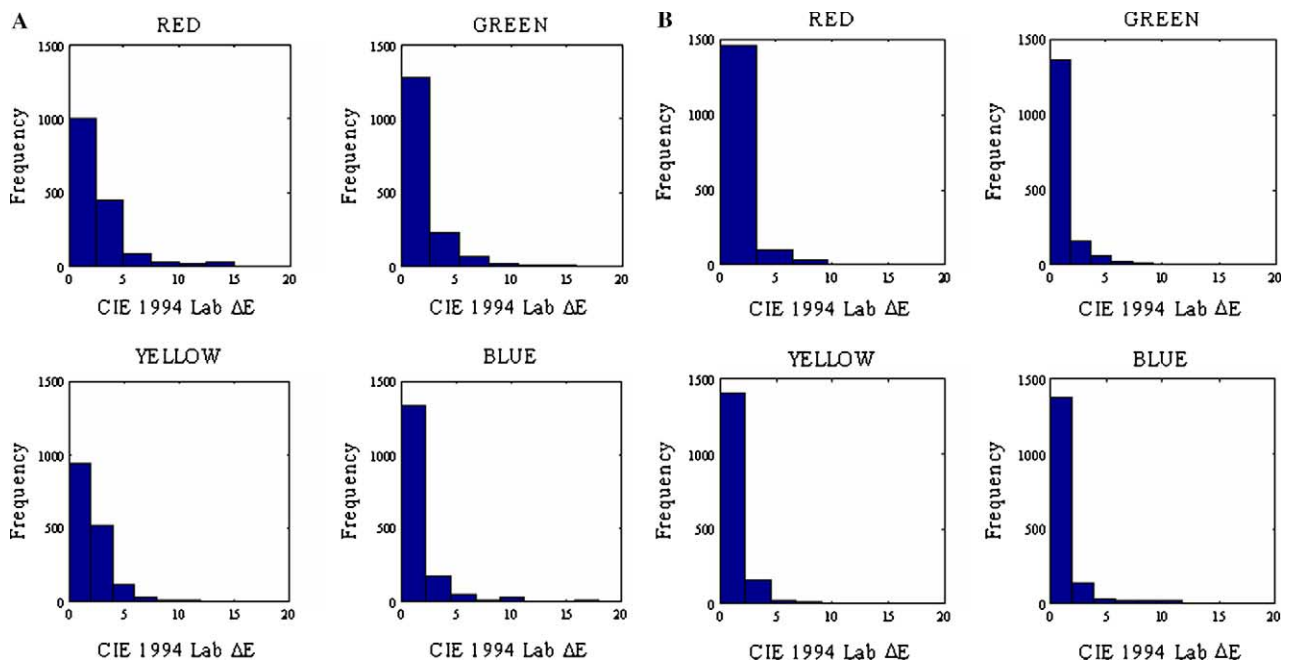


Fig. 4. (A) Error histogram for pooled data for the four unique hues. The frequency of perceptual errors (CIE 1994 Lab ΔE) between the predicted and the observed unique hues are shown for all four unique hues. For all four unique hues almost all errors are below 5 ($n = 1616$). A perceptual error of 5 is visible in side-by-side image comparisons (Engel drum & Ingraham, 1990). (B) Error histogram for individually fitted data. The frequency of perceptual errors (CIE 1994 Lab ΔE) between the predicted and the observed unique hues are shown for all four unique hues; the planes were fitted for each observer individually and the perceptual errors were calculated from the individual predictions. The errors for the individual fits are slightly smaller than for the fits based on the pooled data and most errors are below 3 ($n = 1616$).

compared with uniquely green. In contrast, when a single plane is fitted to unique yellow and unique blue (YB), the average perceptual error is very similar to the errors for the separate fits (Y, B). This is consistent with the hypothesis that unique yellow and unique blue are generated by silencing a single red–green mechanism (cf. Table 1 and Figs. 3(C) and (D)).

4. Discussion

Our aim was to characterise the neural mechanisms that yield the four unique hues: red, green, yellow and blue. In our analysis we did not assess the cone inputs to the unique hues directly, but we determined which chromatic mechanisms are silenced by the four unique hues respectively. Characterising the *null planes* for each unique hue is in the spirit of the original opponent-process theory (Hering, 1964; Hurvich & Jameson, 1957; Larimer et al., 1974; Larimer et al., 1975). The idea of colour-opponent mechanisms are based on Hering's observation that there are colours that contain neither red nor green; these colours are therefore the unique yellow and unique blue hues. Similarly, if yellow and blue are the endpoints of a putative yellow–blue opponent colour channel, then there are colours for which this channel has zero output; these colours that are void of any yellow or blue are therefore called the unique red and unique green hues. The unique hues are therefore defined by nulling the output of particular chromatic mechanisms. Given this operational definition of unique hues, namely via hue cancellation (Hurvich & Jameson, 1957), each unique hue is not a single point in a three-dimensional space. Consider, for instance, unique red: in a space defined by hue, saturation and brightness, there are unique reds at different levels of saturation and different levels of brightness. When plotted in three-dimensional LMS cone space, the unique red data therefore occupy a plane (or another surface) in this three-dimensional space. Our approach was to find the plane such that all unique red data are points on this plane; and similarly for unique yellow, blue, and green. The orientation of this null plane, that is, the vector normal to this null plane, describes the cone inputs to the chromatic mechanism that is silenced by a particular hue (cf. Fig. 3 and Table 1). We have shown that unique yellow and unique blue are generated by a single red–green opponent mechanism; to account for unique red and green we need to postulate two yellow–blue mechanisms with different S cone inputs.

4.1. Non-linearity of the yellow–blue equilibria

The linearity of the yellow–blue mechanism (which implies that unique red and unique green lie on a single

line in a cone-opponent diagram; cf. Fig. 1) has also been explicitly tested and rejected using cone-isolating stimuli (Burns, Elsner, Pokorny, & Smith, 1984a; Knoblauch & Shevell, 2001). Knoblauch and Shevell (2001) fixed the L cone excitation and the observer's task was to adjust the S cone excitation of a given stimulus such the stimulus appeared 'neither yellowish nor bluish'. Plotting the required S cone excitation as a function of the L cone excitation reveals a non-monotonicity in the yellow–blue equilibria (Fig. 4; Knoblauch & Shevell, 2001): initially an increasing amount of S cone excitation is required to compensate for the increase in L cone excitation, indicating that S and L cones contribute in an antagonistic fashion to the yellow–blue equilibria. At a certain L cone level, however, a decreasing amount of S cone excitation is required with an increasing L cone level to obtain a yellow–blue equilibrium (Fig. 4; Knoblauch & Shevell, 2001). This non-monotonicity is inconsistent with a single, linear yellow–blue equilibrium mechanism. A similar direct violation of monotonicity is apparent in the experiments by Burns et al. (1984a); (replotted in Fig. 6, Knoblauch & Shevell, 2001). When Burns' data are replotted in the MacLeod-Boynton diagram (S/(L+M) vs. L/(L+M)); MacLeod & Boynton, 1979) a non-monotonic function (first increasing, then decreasing) is obtained for yellow–blue equilibria, peaking at the neutral background (Illuminant C; L/L+M = 0.65, L/L+M = 0.018). Hence, with an increase in L/L+M cone level, initially an *increasing* amount of S/L+M cone input is inquired; however, when the L/L+M of the test stimulus is larger than the L/L+M coordinate of the neutral grey background (changing from a greenish to a reddish colour appearance), a *decreasing* amount of S/L+M cone input is required to obtain yellow–blue equilibrium. This is exactly the non-monotonicity shown in Fig. 1. Here, we plot the unique hue co-ordinates in a cone-opponent space (DKL space; Derrington et al., 1984) as increments with respect to the neutral grey background (indicated by 0,0). For stimuli of equal luminance with the background (Burns et al., 1984a) the MBL diagram is almost identical (up to a scaling factor and a shift in the origin) to the DKL diagram, since all S and L cone excitations are divided by the same 'L+M' factor when plotted in the MBL diagram. Fig. 1 implies that the S-cone-input is first increasing and then decreasing as a function of the incremental L–M component. For a given luminance level, when the L–M increment is negative (greenish colour appearance) then the S-cone-input needs to be increased to obtain a yellow–blue equilibrium; when the L–M increment is positive (reddish colour) then the S-cone-input needs to be decreased. Webster et al. show qualitatively the same non-monotonicity (Fig. 4, Webster et al., 2000b) as shown in our Fig. 1. We can make quantitative comparisons by

scaling our data according to the method used by Webster et al. (2000b, p. 1547), who used threshold units instead of the scaling described in our Eq. (1). If we apply the same scaling to our data (Fig. 1), the angles of the unique hues in relation to the underlying cone-opponent axes are well within the error of Webster et al.'s data (Table 1, Webster et al., 2000b): our mean angle for unique red is -6.1 , Webster's: 5.4 with a range of -9 to 12.3 ; our unique blue angle is 138.1 , Webster's: 144.6 ranging from 121.0 to 163.3 ; our unique green angle is 207.3 , Webster's: 205.1 ranging from 172.6 to 241.1 ; our unique yellow angle is -51.3 , Webster's: -50.3 ranging from -70.6 to -31.3 . The only hue where we find a slight deviation from Webster's data is unique red, which shows a clear negative angle in our data (hence requiring a negative S cone input); whereas Webster's data suggest that the angle is close to zero. The data from Burns et al. (1984a) are consistent with our data showing a clear negative angle for unique red. Using a very different task, namely hue scaling (Abramov & Gordon, 1994; De Valois et al., 1997), found exactly the same deviations of linearity for unique red and unique green as shown in Fig. 1: unique green lies significantly below the L–M axis (hence requiring negative S cone input) whereas unique red lies closer to the L–M axis (see Fig. 4, De Valois et al., 1997). De Valois et al. (1997) also report a larger variability for red than for green, which could in part explain the slight discrepancies between different studies in the unique red settings. However, the basic non-linearity of the yellow–blue equilibrium mechanism is clearly shown in all discussed data sets; the co-linearity of unique red and unique green is always violated (cf. Fig. 1). Further quantitative comparisons of our data with Webster et al. show a remarkable agreement in the average unique hue settings despite different tasks (hue selection versus hue cancellation). Our results therefore provide further support to the hypothesis that the two higher-order colour mechanisms that yield unique red and unique green respectively combine the incremental and decremental responses of the subcortical chromatic mechanisms with different weights.

4.2. Inter-observer variability

We have shown that the inter-observer variability in the unique hue mechanisms is relatively small when expressed in terms of a perceptual error measurement (CIE, 1995; Zhu et al., 2000). Here, we try to evaluate whether the variability found in our study is in line with previously reported estimates.

In early studies, usually monochromatic lights were used to obtain unique hue settings (e.g., Jameson & Hurvich, 1955; Jordan & Mollon, 1995; Nerger, Volbrecht, & Ayde, 1995; Shefrin & Werner, 1990) and the variability is reported in wavelength. Usually, observers

were dark-adapted and the lights were presented against a dark field. More recently, most unique hues studies used CRTs (e.g., Chichilnisky & Wandell, 1999; Knoblauch & Shevell, 2001; Webster et al., 2000b; Webster et al., 2002) and observers were adapted to a neutral background of moderate luminance (usually > 30 cd/m²). Variability in unique hue settings is sometimes expressed as a hue angle in cone-opponent space, which is either scaled in terms of cone contrast (De Valois et al., 1997) or in terms of threshold (Webster et al., 2000b). A third group of studies used colour chips, such as Munsell Chips, to assess the unique hues (e.g., Kuehni, 2001). In this case the illumination may affect the settings (Kuehni, 2001). By re-analysing our data in terms of hue angles (see above section), we have already shown that our average unique hue loci are well within the error of the settings obtained in a CRT-based study (Webster et al., 2000b).

To allow a comparison with CRT-based data as well as unique hue settings obtained with spectral lights, we also calculated the dominant wavelength (average and range) of the unique hue co-ordinates found in our study. An excellent summary of the experimental unique hue variability in 10 sets of data is provided by Kuehni (2004, Table 1). Table 1 (Kuehni, 2004) shows that the wavelength range (in nm) for unique yellow is rather small (about 20), ranging from about 568 to 589; our settings are slightly lower, with a mean of 571 and a range of 569–581. The range for unique blue is larger than for unique yellow (about 40), from 455 to 495; our mean (range) is 467 (451–482). Unique green is known to have a large spread in wavelength; in the studies reviewed by Kuehni the settings range from 487 to 567; in comparison our mean (range) is 542 (483–563). There are very few wavelengths data available for unique red because of the overlap of unique red into the nonspectral region, which makes a comparison with previous studies difficult. However, where a comparison with previous studies is possible, we find no evidence that the variability exhibited by our observers is significantly smaller than previously reported estimates of variability (cf. Kuehni, 2004; Table 1).

We therefore argue that we reach a slightly different conclusion from some previously published reports, because of the way we express the variability in the unique hue settings. Instead of comparing the variability in wavelength, we use a perceptual measure that takes into account the different sensitivities in different wavelength regions (CIE, 1995; Zhu et al., 2000). This distance measure computes distances in an approximately uniform colour space and therefore reflects the differential sensitivities in different regions of CIE space. When we express the model deviations in this perceptually uniform colour space (cf. Fig. 5), we find that the chromatic tuning of the unique hue mechanisms derived from our data

is very similar when we model each observer individually or when we pool the data across all observers. The additional error arising from pooling the data across all observers is on average only about 1.5 times the average individual error (cf. Fig. 5) and well below the critical perceptual error of about 5 (Engeldrum & Ingraham, 1990). This suggests, at least for these particular colour appearance judgements, a remarkable agreement across colour-normal observers, which is consistent with the hypothesis that the colour vision system in adult humans is able to recalibrate itself based on prior visual experience (Neitz, Carroll, Yamauchi, Neitz, & Williams, 2002). Such an invariance of colour categories across observers may play an important role when we try to communicate the colour of an object verbally.

4.3. Unique hues, sub-cortical and cortical colour tuning

The question how the chromatic unique-hue mechanisms (two yellow–blue mechanisms and one red–green mechanism; cf. Table 1 and Fig. 1) relate to other commonly used red–green and yellow–blue opponent channels is still unresolved. Our experiments shed some light on the neuronal basis of the unique hues.

Our experiment confirms previous findings that the loci of the four unique hues do not coincide with the cardinal cone-opponent axes, as illustrated in Fig. 1 (Burns et al., 1984b; De Valois et al., 1997; Krauskopf et al., 1982; Valberg, 1971; Webster et al., 2000b). The cardinal axes describe the chromatic tuning for neurones in the early visual pathway, namely in the Lateral Geniculate Nucleus (De Valois et al., 2000; Derrington et al., 1984). We quantified the deviation from the cardinal opponent axes by determining the first principal component for each unique hue; they are shown as black lines in Fig. 1. The first eigenvector for red is: 0.0105, -0.0029 , showing a small negative $S-(L+M)$ contribution; for green it is 0.0110, -0.0039 showing a larger and also negative $S-(L+M)$ contribution. The eigenvectors for yellow and blue are -0.0134 , 0.0103 and 0.0144, -0.0102 respectively, demonstrating a roughly equal contribution of $L-M$ and $S-(L+M)$ for both unique hues. Hence, the unique hues are clearly not computed by neurones with chromatic tuning found in the Lateral Geniculate Nucleus. Equating the cone-opponent mechanisms found in the LGN with the unique hues is an often repeated misperception and seems to be propagated despite an overwhelming amount of evidence to the contrary.

Neurones in visual cortex have very different chromatic signatures than the parvocellular neurones found in the Lateral Geniculate Nucleus (De Valois et al., 2000; Johnson et al., 2001; Kiper et al., 1997; Lennie et al., 1990). The majority of cortical neurones are tuned to other than the cardinal directions, but there is no significant subset of neurones tuned to the colour direc-

tions that define the unique hues (cf. Fig. 1). However, De Valois and De Valois (1993) propose higher-order cortical colour mechanisms that are consistent, at least qualitatively, with the red–green and yellow–blue mechanisms derived with our hue selection task. Firstly, all three chromatic mechanisms, derived via our hue selection task, receive an LM cone-opponent input (cf. Figs. 3(A)–(D)) as proposed by De Valois and De Valois (1993). The single red–green mechanism, derived from the unique yellow and blue data, receives $L-M$ input and an S cone input (cf. Figs. 3(C) and (D); Table 1). In De Valois's third colour processing stage, the red and green poles of the perceptual colour axes all receive an $L-M$ opponent input. But their yellow–blue mechanism also takes linear combinations of an $L-M$ component and an S cone component. The two YB mechanisms (derived from the unique red and green data) are also linear combinations of an $L-M$ opponent input and an S cone input (cf. Figs. 3(A) and (B); Table 1). Although quantitative comparisons are difficult due to the different scale factors applied in both studies, it is encouraging that psychophysical hue cancellation experiments and neurophysiological recordings in visual cortex arrive at the same basic conclusions.

Acknowledgments

This study was supported by an EPSRC Grant (EP/C000404/1) awarded to SMW. We thank Jesus Malo for his assistance in the dominant wavelength calculations.

References

- Abramov, I., & Gordon, J. (1994). Color appearance: On seeing red or yellow, or green, or blue. *Annual Review of Psychology*, 45, 451–485.
- Barbur, J. L., Harlow, A. J., & Plant, G. T. (1994). Insights into the different exploits of color in the visual-cortex. *Proceedings of the Royal Society of London Series B-Biological Sciences*, 258(1353), 327–334.
- Brainard, D. (1996). Cone contrast and opponent modulation color spaces. In Kaiser & Boynton (Eds.), *Human Color Vision* (pp. 563–579). Washington, DC: Optical Society of America.
- Burns, S. A., Elsner, A. E., Pokorny, J., & Smith, V. C. (1984a). The abney effect: Chromaticity coordinates of unique and other constant hues. *Vision Research*, 24(5), 479–489.
- Burns, S. L., Elsner, A. E., Pokorny, J., & Smith, V. C. (1984b). The Abney effect: Chromaticity coordinates of unique and other constant hues. *Vision Research*, 24, 479–489.
- Chichilnisky, B. A., & Wandell, B. A. (1999). Trichromatic opponent color classification. *Vision Research*, 39, 3444–3458.
- Cicerone, C., Krantz, D., & Larimer, J. (1975). Oponent-process additivity. III: Effect of moderate chromatic adaptation. *Vision Research*, 15, 1125–1135.
- CIE (1995). Industrial color-difference evaluation, CIE Publ. No. 116. (Vienna, Austria: Central Bureau of the CIE).
- De Valois, R. L., & De Valois, K. K. (1993). A multi-stage color model. *Vision Research*, 33(8), 1053–1065.

- De Valois, R. L., Cottaris, N. P., Elfar, S. D., Mahon, L. E., & Wilson, J. A. (2000). Some transformations of color information from lateral geniculate nucleus to striate cortex. *Proceedings of the National Academy of Sciences of the United States of America*, 97(9), 4997–5002.
- De Valois, R. L., De Valois, K. K., Switkes, E., & Mahon, L. E. (1997). Hue scaling of isoluminant and cone-specific lights. *Vision Research*, 37, 885–897.
- Derrington, A. M., Krauskopf, J., & Lennie, P. (1984). Chromatic mechanisms in lateral geniculate nucleus of macaque. *Journal of Physiology*, 357, 241–265.
- Engel drum, P. G., & Ingraham, J. L. (1990). Analysis of white point and phosphor set differences of CRT displays. *Color Research and Application*, 15(3), 151–155.
- Gegenfurtner, K. R., Kiper, D. C., & Levitt, J. B. (1997). Functional properties of neurons in macaque area V3. *Journal of Neurophysiology*, 77(4), 1906–1923.
- Helmholtz, H. (2000). *Treatise on Physiological Optics* (1896). (Thoemmes).
- Hering, E. (1964). *Outlines of a theory of the light sense*. Cambridge: Massachusetts: Harvard University Press.
- Hurvich, L., & Jameson, D. (1955). Some quantitative aspects of an opponent-color theory. II. Brightness, saturation, and hue in normal and dichromatic vision. *Journal of the Optical Society of America*, 45, 602–616.
- Hurvich, L., & Jameson, D. (1957). An opponent-process theory of color vision. *Psychological Review*, 64, 384–404.
- Ikeda, M., & Ayama, M. (1980). Additivity of opponent chromatic valence. *Vision Research*, 20, 995–999.
- Ingling, C. R., Russell, P. W., Rea, M. S., & Tsou, B. H. (1978). Red-green opponent spectral sensitivity: Disparity between cancellation and direct matching methods. *Science*, 201, 1221–1223.
- Jameson, D., & Hurvich, L. (1955). Some quantitative aspects of an opponent-colors theory. I. Chromatic responses and spectral saturation. *Journal of the Optical Society of America*, 45, 546–552.
- Jobson, J. D. (1991). *Applied multivariate data analysis, Vols. 1 and 2*. New York: Springer.
- Johnson, E. N., Hawken, M. J., & Shapley, R. (2001). The spatial transformation of color in the primary visual cortex of the macaque monkey. *Nature Neuroscience*, 4(4), 409–416.
- Jordan, G., & Mollon, J. D. (1995). Rayleigh matches and unique green. *Vision Research*, 35, 613–620.
- Kiper, D. C., Fenstemaker, S. B., & Gegenfurtner, K. R. (1997). Chromatic properties of neurons in macaque area V2. *Visual Neuroscience*, 14(6), 1061–1072.
- Knoblauch, K., & Shevell, S. K. (2001). Relating cone signals to color appearance: Failure of monotonicity in yellow/blue. *Visual Neuroscience*, 18(6), 901–906.
- Knoblauch, K., Sirovich, L., & Wooten, B. R. (1985). Linearity of hue cancellation in sex-linked dichromacy. *Journal of the Optical Society of America*, 2(2), 136–146.
- Krauskopf, J., Williams, D. R., & Heeley, D. W. (1982). Cardinal directions of colour space. *Vision Research*, 22, 1123–1131.
- Kuehni, R. G. (2001). Determination of unique hues using munsell color chips. *Color Research and Application*, 26(1), 61–66.
- Kuehni, R. G. (2004). Variability in unique hue selection: A surprising phenomenon. *Color Research and Application*, 29(2), 158–162.
- Larimer, J., Krantz, D., & Cicerone, C. (1974). Opponent-process additivity. I: Red/green equilibria. *Vision Research*, 14, 1127–1140.
- Larimer, J., Krantz, D., & Cicerone, C. (1975). Opponent-process additivity. II: Yellow/blue equilibria and nonlinear models. *Vision Research*, 15, 723–731.
- Lee, T.-W., Wachtler, T., & Sejnowski, T. J. (2002). Color opponency is an efficient representation of spectral properties in natural scenes. *Vision Research*, 42(17), 2095–2103.
- Lennie, P., Krauskopf, J., & Schlar, G. (1990). Chromatic mechanisms in striate cortex of macaque. *Journal of Neuroscience*, 10, 649–669.
- MacLeod, D. I. A., & Boynton, R. M. (1979). Chromaticity diagram showing cone excitation by stimuli of equal luminance. *Journal of the Optical Society of America*, 69, 1183–1186.
- Maloney, L. T., Wuerger, S. M., & Krauskopf, J. (1994). A method for testing Euclidean representations of proximity judgments in linear psychological spaces. In H. D'Zmura, Iverson, & Romney (Eds.), *Geometric Representations of Perceptual Phenomena* (pp. 137–152). Hillsdale: New Jersey: Lawrence Erlbaum.
- Mausfeld, R., & Niederee, R. (1993). A inquiry into relational concepts of colour, based on incremental principles of colour coding for minimal relational stimuli. *Perception*, 22(4), 427–462.
- Mollon, J. D. (1991). Uses and evolutionary origins of primate color vision. In: J.R.A.G. Cronly-Dillon, R.L. (Ed.) *Evolution of the eye and visual system (Vision and visual dysfunction) 2*, Boca Rota, FL: CRC Press.
- Mollon, J. D., & Jordan, G. (1997). On the nature of unique hues. In I. M. D. C. C. Dickinson (Ed.), *John Daltons colour vision legacy* (pp. 381–392). London: Taylor and Francis.
- Morita, T., Kochiyama, T., Okada, T., Yonekura, Y., Matsumura, M., & Sadato, N. (2004). The neural substrates of conscious color perception demonstrated using fMRI. *Neuroimage*, 21(4), 1665–1673.
- Neitz, J., Carroll, J., Yamauchi, Y., Neitz, M., & Williams, D. R. (2002). Color perception is mediated by a plastic neural mechanism that is adjustable in adults. *Neuron*, 35, 783–792.
- Nerger, J. L., Volbrecht, V. J., & Ayde, C. J. (1995). Unique hue judgments as a function of test size in the fovea and at 20-deg temporal eccentricity. *Journal of the Optical Society of America a-Optics Image Science and Vision*, 12(6), 1225–1232.
- Purves, D., Lotto, B., & Polger, T. (2000). Color vision and the four-color-map problem. *Journal of Cognitive Neuroscience*, 12(2), 233–237.
- Saunders, B. A. C., & van Brakel, J. (1997). Are there nontrivial constraints on colour categorization? *Behavioral and Brain Sciences*, 20(2), 167.
- Scheffrin, B. E., & Werner, J. S. (1990). Loci of spectral unique hues throughout the life-span. *Journal of the Optical Society of America a-Optics Image Science and Vision*, 7(2), 305–311.
- Sheffrin, B. E., & Werner, J. S. (1990). Loci of spectral unique hues throughout the life span. *Journal of the Optical Society of America A*, 7, 305–311.
- Travis, D. (1991). *Effective color displays. Computers and people series*. London: Academic Press.
- Valberg, A. (1971). A method for the precise determination of achromatic colours including white. *Vision Research*, 11, 157–160.
- Valberg, A. (2001). Unique hues: An old problem for a new generation. *Vision Research*, 41(13), 1645–1657.
- Wachtler, T., Sejnowski, T. J., & Albright, T. D. (2003). Representation of color stimuli in awake macaque primary visual cortex. *Neuron*, 37(4), 681–691.
- Wandell, B. A., Poirson, A. B., Newsome, W. T., Baseler, H. A., Boynton, G. M., Huk, A., Gandhi, S., & Sharpe, L. T. (1999). Color signals in human motion-selective cortex. *Neuron*, 24(4), 901–909.
- Webster, M. A., Miyahara, E., Malkoc, G., & Raker, V. E. (2000a). Variations in normal color vision. I. Cone-opponent axes. *Journal of the Optical Society of America A*, 17(9), 1535–1544.
- Webster, M. A., Miyahara, E., Malkoc, G., & Raker, V. E. (2000b). Variations in normal color vision. II. Unique hues. *Journal of the Optical Society of America A*, 17(9), 1545–1555.

- Webster, M. A., Webster, S. M., Bharadwaj, S., Verma, R., Jaikumar, J., Madan, G., & Vaithilingham, E. (2002). Variations in normal color vision. III. Unique hues in Indian and United States observers. *Journal of the Optical Society of America A – Optics Image Science and Vision*, 19(10), 1951–1962.
- Werner, J. S., & Wooten, B. R. (1979). Opponent chromatic mechanisms: Relation to photopigments and hue naming. *Journal of the Optical Society of America*, 69(3), 422–434.
- Wuerger, S. M. (1996). Colour appearance changes resulting from isoluminant chromatic adaptation. *Vision Research*, 36(19), 3107–3118.
- Wuerger, S. M., Maloney, L. T., & Krauskopf, J. (1995). Proximity judgments in colour space: Test of a Euclidean colour geometry. *Vision Research*, 35(6), 827–835.
- Wuerger, S. M., Watson, A. B., & Ahumada, A. (2002). Towards a spatio-chromatic standard observer for detection, in Vol., pp. *Human vision and electronic imaging VII*, B.E. Rogowitz and T.N. Pappas (Eds.), Proceedings of SPIE, San Jose, CA, USA, 4662, 159–172.
- Wyszecki, G., & Stiles, W. S. (1982). *Color science: Concepts and methods, quantitative data and formulae*. New York: John Wiley & Sons.
- Zaidi, Q., Yoshimi, B., Flanigan, N., & Canova, A. (1992). Lateral interactions within color mechanisms in simultaneous induced contrast. *Vision Research*, 32(9), 1695–1707.
- Zhu, S. Y., Luo, M. R., & Cui, G. H. (2000). *New experimental data for investigating uniform colour space*. Arizona: CIE Expert Symposium Scotsdale.